

Test of UFSD Silicon Detectors for the TOTEM Upgrade Project

R. Arcidiaconoi¹, M. Berretti², E. Bossini^{4,3},
M. Bozzo⁵, N. Cartiglia⁶, M. Ferrero^{7,6},
V. Georgiev⁸, T. Isidori³, R. Linhart⁸, N. Minafra⁹,
M. M. Obertino⁷, V. Sola⁶, N. Turini^{10,11}

¹ Università degli Studi del Piemonte Orientale, Largo Donegani 1 - 28100 Novara, Italy.

² University of Helsinki and Helsinki Institute of Physics, P.O. Box 64, FI-00014, Helsinki, Finland.

³ Università degli studi di Pisa and INFN di Pisa, Largo B. Pontecorvo 3, 56127 Pisa, Italy.

⁴ Centro Studio e Ricerche Enrico Fermi Piazza del Viminale 1 - 00184 Roma (Italy).

⁵ INFN Sezione di Genova, Via Dodecaneso 33, 16136 Genova, Italy.

⁶ Sezione INFN di Torino, Via P.Giuria, 1 - 10125 Torino, Italy.

⁷ Università degli Studi di Torino, Via P.Giuria, 1 - 10125 Torino, Italy

⁸ University of West Bohemia, Pilsen, Univerzitni 8, PILSEN 30614 (Czech Republic).

⁹ University of Kansas, 1246 West Campus Road, Lawrence - KS 66045, USA.

¹⁰ Università degli Studi di Siena and Gruppo Collegato INFN-Siena, Via Roma 56, 53100 Siena, Italy.

¹¹ CERN, Geneva, Switzerland.

February 20, 2017

Abstract This paper describes the performance of a prototype timing detector, based on 50 μm thick Ultra Fast Silicon Detector, as measured in a beam test using a 180 GeV/c momentum pion beam. The dependence of the time precision on the pixel capacitance and the bias voltage is investigated here. A timing precision from 30 ps to 100 ps, depending on the pixel capacitance, has been measured at a bias voltage of 180 V. Timing precision has also been measured as a function of the bias voltage.

PACS Keywords: Picoseconds, Timing detectors, LGAD, UFSD, Silicon detectors, LHC, Amplifier

PACS: 29.40.Wk, 29.40.Gx

1 Timing Detector for the TOTEM Proton Time of Flight Measurement at the LHC

The TOTEM experiment will install new timing detectors to measure the time of flight (TOF) of protons produced in central diffractive (CD) collisions at the LHC [1].

The CD interactions measured by TOTEM at $\sqrt{s} = 13$ TeV are characterized by having two high energy protons (with momentum greater than 5 TeV) scattered at less than 100 μrad from the beam axis. In the presence of pile-up¹ events the reconstruction of the protons interaction vertex position allows to associate the physics objects reconstructed by the CMS experiment with the particles generated from that vertex. The TOF detectors installed in the TOTEM Roman Pots (RPs)² will measure with high precision the arrival time of the CD

^aCorresponding author's e-mail: mirko.berretti@cern.ch

¹Probability that more than one interaction is produced during the same bunch crossing.

²Special movable insertion in the LHC vacuum beam pipe that allow to move a detector edge very close to the circulating beam.

protons on each side of the interaction point. They will operate in the LHC with a scenario of moderate pile-up ($\mu \sim 1$) and a time precision of at least 50 ps per arm is required to efficiently identify the event vertex [2]. Since the difference of the arrival times is directly proportional to the longitudinal position of the interaction vertex ($z_{VTX} = c\Delta t/2$), a precision of 50 ps will allow to know the longitudinal interaction vertex position to less than 1 cm.

The timing detector will be installed in four vertical RPs located at 210 m from the interaction point 5 (IP5) of the LHC. The detector comprises four identical stations, each consisting of four hybrid boards³ equipped either with an ultra fast silicon detector (UFSD) [3], [4], [5],[6] or with a single crystal chemical vapor deposition (scCVD) diamond sensor [7], [8]. The board contains 12 independent amplifiers, each bonded to a single pad (pixel) of the sensors. The typical time precision of one plane equipped with scCVD is in the range of 50 100 ps, while it is in the 30 100 ps range for one equipped with an UFSD sensor. Combining TOF measurements from 4 detector planes will provide an ultimate time precision better than ~ 50 ps, which translates in a precision on the longitudinal position of the interaction vertex $\sigma_z < 1$ cm.

2 Ultra Fast Silicon Detector

Ultra Fast Silicon Detectors, a new concept in silicon detector design, associate the best characteristics of standard silicon sensors with the main feature of Avalanche Photo Diodes (APD).

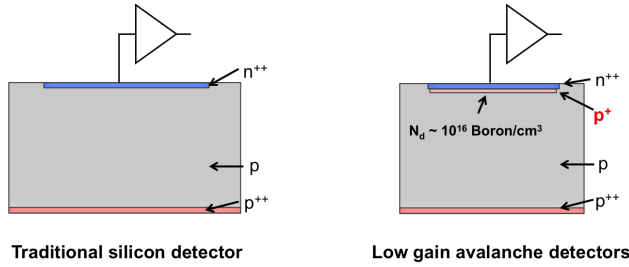


Fig. 1 Comparison of the structures of a silicon diode (left) and a Low-Gain Avalanche Diode (right). The additional p^+ layer near the n^{++} electrode creates, when depleted, a large electric field that generates charge multiplications.

UFSD are thin (typically $50\mu\text{m}$ thick) silicon Low Gain Avalanche Diodes (LGAD) [9], [10], that produce large signals showing hence a large dV/dt , a characteristic necessary to measure time accurately.

Charge multiplication in silicon sensors happens when the charge carriers drift in electric fields of the order of $E \sim 300 \text{ kV/cm}$. Under this condition the drifting electrons acquire sufficient kinetic energy to generate additional e/h pairs. A field value of 300 kV/cm in a semiconductor can be obtained by implanting an appropriate charge density around $N_D \sim 10^{16} / \text{cm}^3$, that will locally generate the required very high fields. Indeed in the LGAD design (Figure 1) an additional doping layer is added at the $n-p$ junction which, when fully depleted, generates the high field necessary to achieve charge multiplication. Gain depends

³The particle sensor and the amplification electronic are mounted on the same PCB.

exponentially on the value of the electric field E , $N(l) = N_0 e^{\alpha(E)l}$, where α is a strong function of E and l is the mean path length in the high field region.

First results of time resolution of thin LGADs (UFSD), and based on beam test measurements, have been published in 2016 [11].

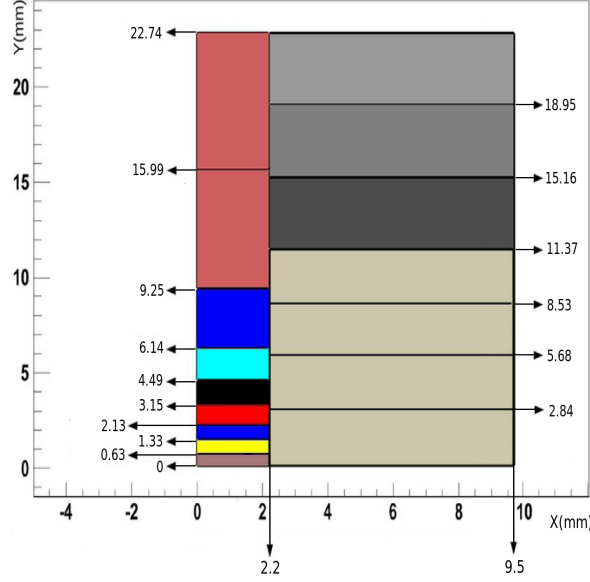


Fig. 2 Sensor geometry of the TOTEM UFSD prototype made up of 15 pixels of different dimensions.

Radiation tolerance studies have shown [12], [13] that LGAD sensors can withstand up to $10^{14} n_{eq}/cm^2$ without loss of performance.

LGAD sensors can be built in many sizes and shapes, ranging from thin strips to large pads. The measurements reported here have been performed on a 2 cm^2 $50\mu\text{m}$ thick UFSD sensor, manufactured by CNM⁴ with a structure specifically designed for the TOTEM experiment, mounted on a standard TOTEM hybrid board [7].

3 Description of the UFSD-based Timing Board

The UFSD sensor used for the prototype timing plane has 15 pixels with the pixel layout shown in Figure 2.

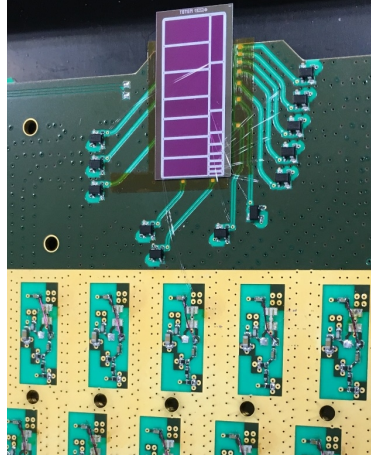
Prior to the gluing of the sensor on the hybrid board, each of the 15 pixels had been tested in the lab to determine its maximum operating voltage.

Only pixels with a breakdown voltage higher than 180 V and a leakage current lower than 0.1 mA, were bonded to the amplification channel by means of standard $25\mu\text{m}$ aluminum wires (Figure 3).

⁴Centro Nacional de Microelectrónica, Campus Universidad Autónoma de Barcelona. 08193 Bellaterra (Barcelona), Spain.

Table 1 Characteristics of the 50 μm UFSD pixels used in the tests.

Pixel N	Surface [mm ²]	Capacitance [pF]	Preamplifier feedback [ohm]
1	1.8	3.1	1 k
2	2.2	4.4	1 k
3	3.0	6.0	1 k
4	7.0	14	1 k
5	14	28	300

**Fig. 3** The UFSD sensor mounted on the TOTEM hybrid board.

The UFSD output pulse shape simulated with the simulation program Weightfield2⁵, developed particularly for LGAD devices [14], assuming a bias voltage of 200 V and a sensor gain of 10 is shown in Figure 4.

The detector generates a current whose maximum is about 8 μA .

Capacitance of the 50 μm thick UFSD pixels scales linearly with their area as ~ 2 pF/mm²: dimensions and relative capacitance for the pixels measured here are summarized in table 1.

4 Front End Electronics

Given the UFSD intrinsic charge amplification one expects the primary charge presented at the input of the amplifier to be 10-100 times larger than the one expected from a diamond sensor. The TOTEM hybrid, originally designed for scCVD diamonds [7], was modified for the UFSD eliminating the second amplification stage, referred elsewhere as ABA. The amplification chain has now only 3 active elements (one BFP840ESD and two BFG425W BJT transistors). Moreover, since the UFSD pixels have a larger capacitance than diamond sensors, in order to maintain a fast rise time the feedback resistor of the preamplification

⁵open source code may be found at <http://personalpages.to.infn.it/~cartigli/Weightfield2/Main.html>

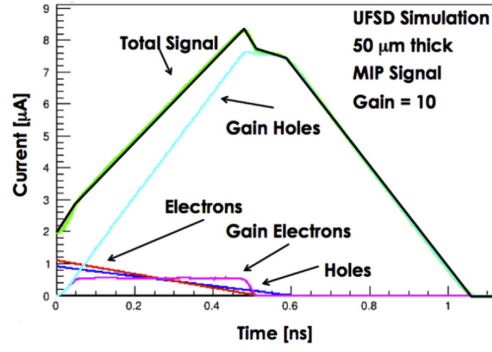


Fig. 4 Simulations of the pulse shape from a 50 μm UFSD with a gain of 10 (from [15]). The plot shows the contribution of each component of the generated charge.

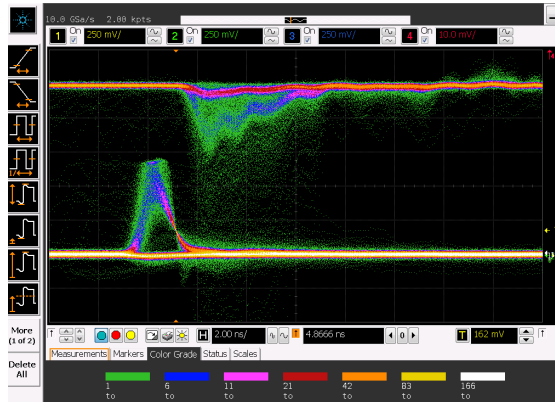


Fig. 5 Event display of several MCP (top) and UFSD (bottom) signals. The oscilloscope record was triggered by the UFSD signal.

chain has been reduced to to $1\text{k}\Omega$ or 300Ω , accordingly to the capacitance of the pixel (see table 1).

5 Test Beam Measurements

The time precision of the UFSD sensors has been measured at the H8 beam line of the CERN SPS, a 180 GeV/c pion beam, by computing the time difference of the signal produced by particles crossing a Micro Channel Plate (MCP) PLANACONTM 85011-501⁶ and one of the UFSD pixels. The particle rate was $\sim 10^3/\text{mm}^2$, the HV on the UFSD was set initially at 180 V, which is the maximum voltage before pixels breakdown, and varied down to 140 V. The maximum current allowed in the present measurement was 0.1 mA. A screen shot from the oscilloscope with the signals from the MCP and the UFSD detectors is shown in Figure 5.

⁶ PLANACONTM Photomultiplier tube assembly 85011-501 from BURLE.

The UFSD pixels that we tested have an area ranging between 1.8 mm^2 and 14 mm^2 . The 2.2 mm^2 UFSD pixel shows an average S/N of ~ 60 (Figure 6) and a risetime of 0.6 ns (Figure 7).

The UFSD S/N curve for the events used in this analysis does not show the typical Landau curve tail; this is due to the saturation of $\sim 10\%$ of the signals and may include the effect of a non linearity in the modified amplification chain.

Signals are recorded with a 20 Gsa/s DSO9254A Agilent oscilloscope. The time difference between the MCP and the 2.2 mm^2 UFSD pixel is shown in Figure 8. The difference is computed off-line by using a constant fraction discrimination with a threshold at 30% of the maximum for both the UFSD and the MCP signal.

The MCP time precision was obtained from other measurements and is $(40 \pm 5) \text{ ps}$.

The results of the measurements are summarized in Table 2.

Figures 9 and 10 show the UFSD time precision as a function of the pixel capacitance and of the applied bias voltage respectively; the second set of measurements was performed on the pixel with an area of 2.2 mm^2 . The precision of the measurement is mainly due to the uncertainty with which we know the MCP time precision.

Table 2 Results of the time precision measurements as a function of the pixel capacitance, pixel surface area and of the applied bias Voltage. The uncertainty on the measured values is of $\sim 5 \text{ ps}$ and depends essentially on the uncertainty of the MCP reference measurement.

Surface [mm ²]	Capacitance [pF]	HV [V]	Time precision [ps]
1.8	3.1	180	32
2.2	4.4	180	33
3.0	6.0	180	38
7.0	14	180	57
14	28	180	102
2.2	4.4	140	49
2.2	4.4	160	41
2.2	4.4	180	33

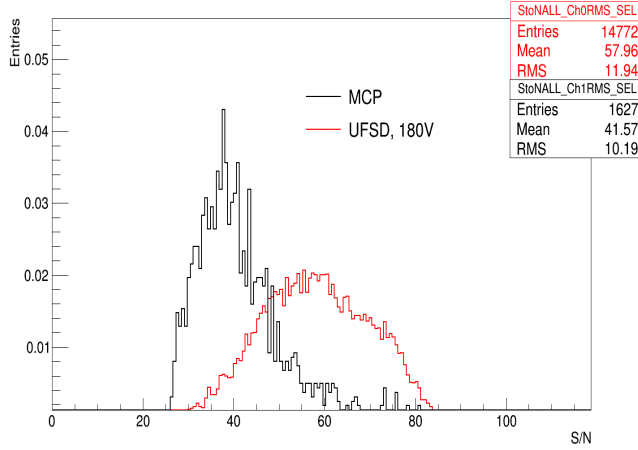


Fig. 6 Signal to Noise ratio of the MCP and of the 2 mm^2 UFSD pixel.

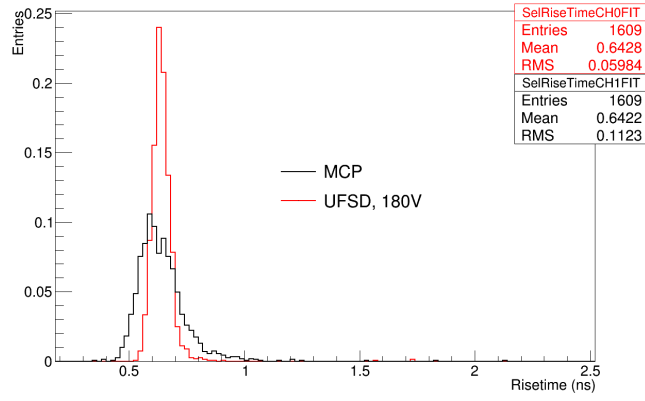


Fig. 7 Risetime of the MCP and of the 2 mm² UFSD pixel.

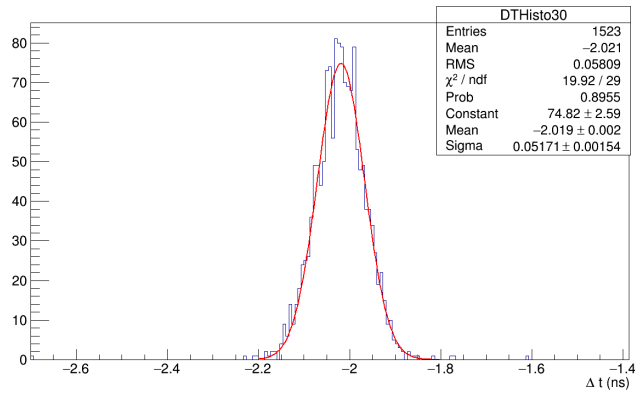


Fig. 8 Difference of the arrival time measured by the MCP and by the 2.2 mm² UFSD pixel biased at 180 V.

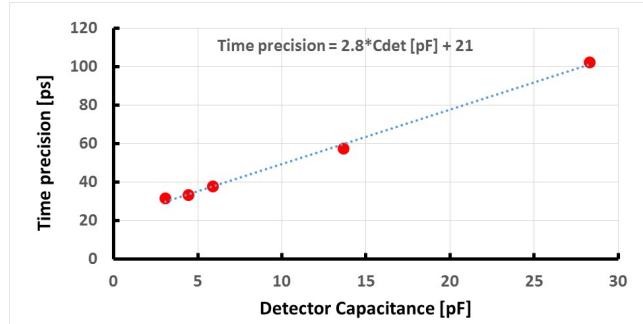


Fig. 9 UFSD time precision as a function of the pixel capacitance for a bias of 180V.

The trend of the measurements suggests that a time precision of less than 30 ps could be reached for the smallest area pixel biased at 200 V.

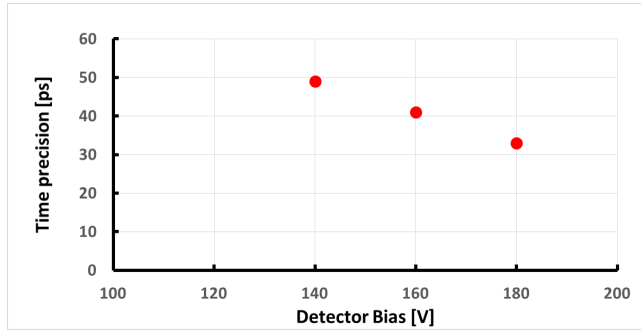


Fig. 10 UFSD time precision (2.2 mm² pixel) as a function of the applied bias Voltage.

6 Conclusions

Here we described the timing performance of a 50 μm thick UFSD detector on a beam of minimum ionizing particles. A time precision in the range of 30-100 ps has been measured, depending on the pixel capacitance. The UFSD technology will be used by TOTEM experiment in the vertical RPs together with scCVD sensors.

Acknowledgments

We thank Florentina Manolescu and Jan McGill for the realization of the unusual bonding of the sensors. Support for some of us to travel to CERN for the beam tests was provided by AIDA-2020-CERN-TB-2016-11. This work was supported by the institutions listed on the front page and also by the project LM2015058 from the Czech Ministry of Education Youth and Sports. Part of this work has been financed by the European Unions Horizon 2020 Research and Innovation funding program, under Grant Agreement no. 654168 (AIDA-2020) and Grant Agreement no. 669529 (ERC UFSD669529), and by the Italian Ministero degli Affari Esteri and INFN Gruppo I and V. The design was supported by National program of sustainability LO1607 Rice-Netesis of the Ministry of Education, Youth and Sports, Czech Republic.

References

1. M. Albrow and others and the CMS-TOTEM Collaboration. CMS-TOTEM Precision Proton Spectrometer. Technical Report CERN-LHCC-2014-021. TOTEM-TDR-003. CMS-TDR-13, Sep 2014.
2. Addendum to the TOTEM TDR: Timing Measurements in the Vertical Roman Pots of the TOTEM Experiment LHCC document CERN-LHCC-2014-020 including questions/answers from/to the referees. Technical Report CERN-LHCC-2014-024. TOTEM-TDR-002-ADD-1, CERN, Geneva, Nov 2014.
3. G.-F. Dalla Betta et al. Design and tcad simulation of double-sided pixelated low gain avalanche detectors. *Nuclear Instruments and Methods, Section A.*, 796:154, 2015. Proceedings of the 10th International Conference on Radiation Effects on Semiconductor Materials Detectors and Devices.
4. H.F-W. Sadrozinski et al. Sensors for ultra-fast silicon detectors. *Nuclear Instruments and Methods, Section A.*, 765:7, 2014. HSTD-9 2013 - Proceedings of the 9th International Hiroshima Symposium on Development and Application of Semiconductor Tracking Detectors - International Conference Center, Hiroshima, Japan, 2 - 5 September 2013.
5. H. F-W. Sadrozinski et al. Ultra-fast silicon detectors. *Nuclear Instruments and Methods, Section A.*, 730:226, 2013. Proceedings of the 9th International Conference on Radiation Effects on Semiconductor

-
- Materials Detectors and Devices; October 9-12 2012 Dipartimento di Fisica e Astronomia - Sezione di Astronomia e Scienza dello Spazio - Largo Enrico Fermi, 2, 50125 Firenze.
6. N. Cartiglia et al. Design optimization of ultra-fast silicon detectors. *Nuclear Instruments and Methods, Section A.*, 796:141, 2015. Proceedings of the 10th International Conference on Radiation Effects on Semiconductor Materials Detectors and Devices.
 7. G. Antchev, et al., Diamond Detectors for the TOTEM Timing Upgrade (CERN-EP-2016-317). [arXiv:1701.05227](#); [cds.cern.ch:2239248](#).
 8. Berretti, M. et al. Timing Performance of a Double Layer Diamond Detector. [arXiv:1612.09140](#), 2016. Submitted to JINST, Dec 2016.
 9. P. Fernández-Martínez et al. Simulation of new p-type strip detectors with trench to enhance the charge multiplication effect in the n-type electrodes. *Nuclear Instruments and Methods, Section A.*, 658(1):98 – 102, 2011. {RESMDD} 2010.
 10. G. Pellegrini et al. Technology developments and first measurements of low gain avalanche detectors (lgad) for high energy physics applications. *Nuclear Instruments and Methods, Section A.*, 765:12 – 16, 2014. HSTD-9 2013 - Proceedings of the 9th International Hiroshima Symposium on Development and Application of Semiconductor Tracking Detectors - International Conference Center, Hiroshima, Japan, 2 - 5 September 2013.
 11. N. Cartiglia et al. Beam test results of a 16 ps timing system based on ultra-fast silicon detectors, [arXiv:1608.08681v3](#), 2016.
 12. B. Baldassarri et al. Signal formation in irradiated silicon detectors. *Nuclear Instruments and Methods, Section A.*, page in print, 2016.
 13. G. Kramberger et al. Radiation effects in low gain avalanche detectors after hadron irradiations. *Journal of Instrumentation*, 10(07):P07006, 2015.
 14. F. Cenna et al. Weightfield2: A fast simulator for silicon and diamond solid state detector. *Nuclear Instruments and Methods, Section A.*, 796:149, 2015. Proceedings of the 10th Int. Conf. on Radiation Effects on Semiconductor Materials Detectors and Devices.
 15. N. Cartiglia et al. Design optimization of ultra-fast silicon detectors. *Nucl. Instrum. Meth.*, A796:141–148, 2015.